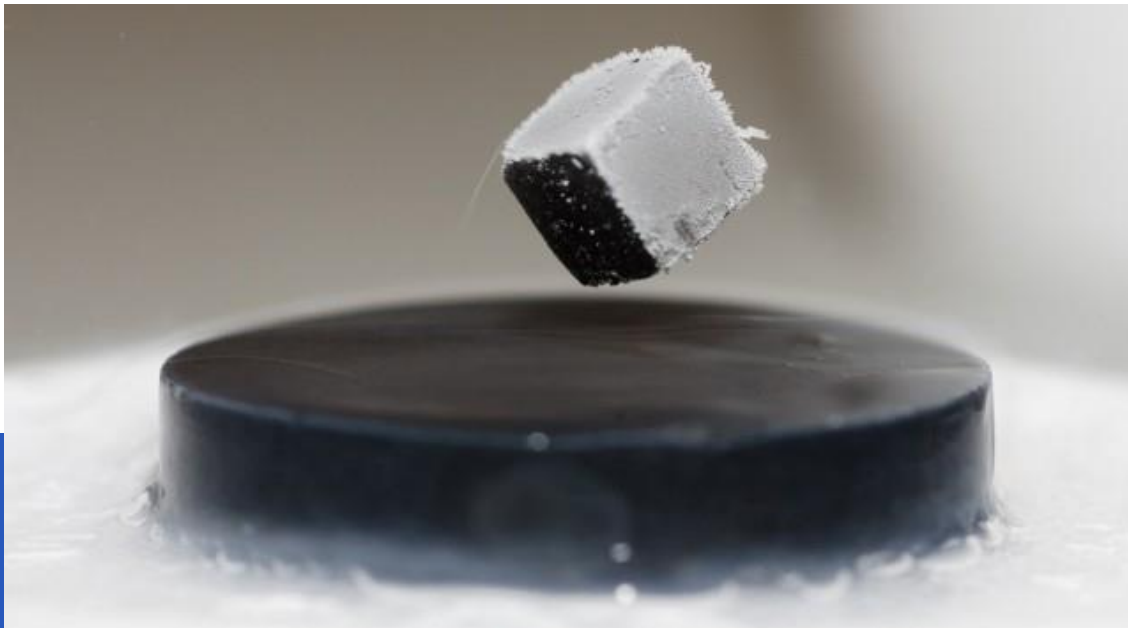
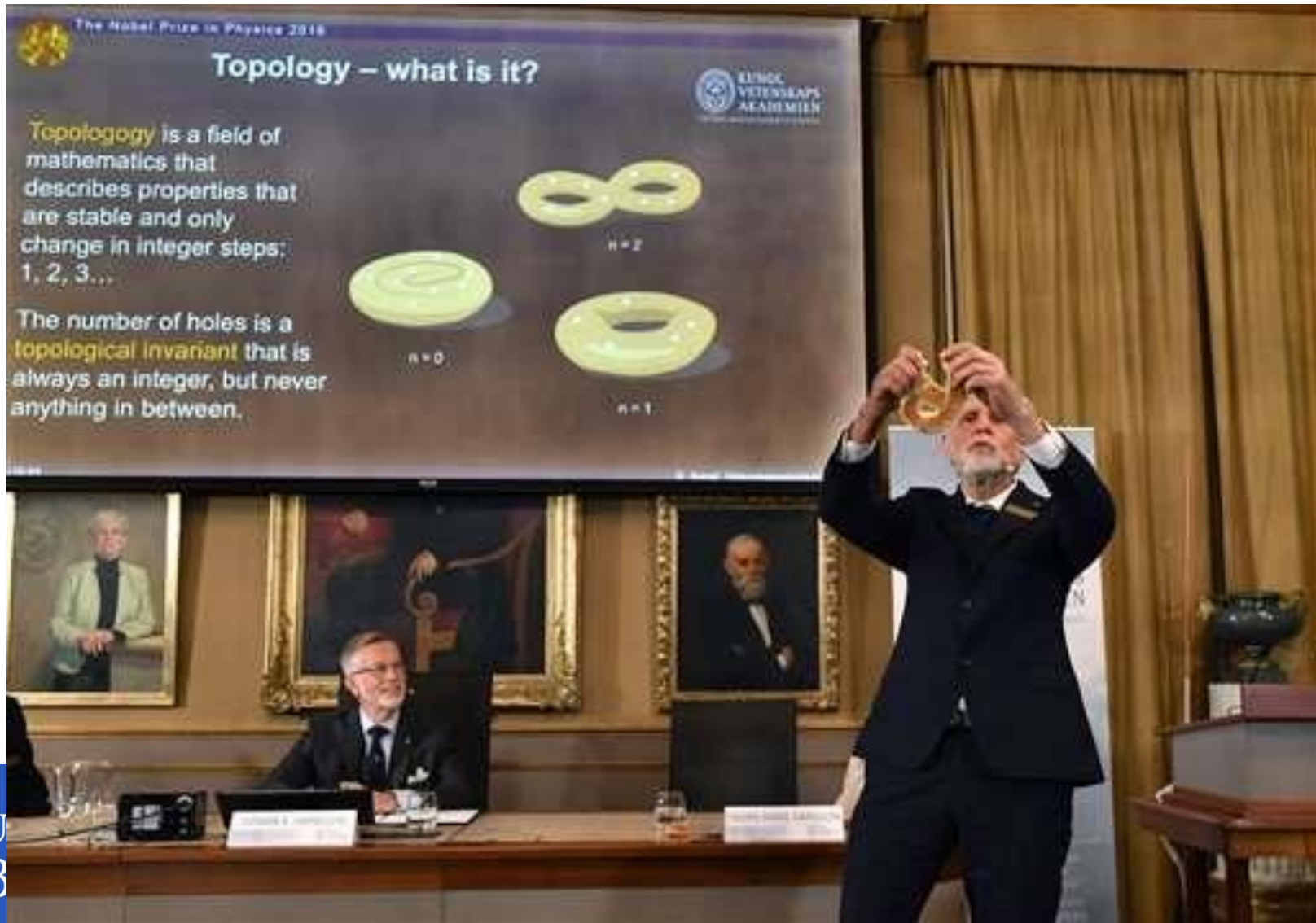




# Topological Superconductivity



# 🌟 Topology in condensed matter physics?



# 2016 Nobel prize for physics

PRESS RELEASE

4 October 2016

## The Nobel Prize in Physics 2016

The Royal Swedish Academy of Sciences has decided to award the Nobel Prize in Physics 2016 with one half to

**David J. Thouless**

University of Washington, Seattle, WA, USA

and the other half to

**F. Duncan M. Haldane**

Princeton University, NJ, USA

and

**J. Michael Kosterlitz**

Brown University, Providence, RI, USA

*“for theoretical discoveries of topological phase transitions and topological phases of matter”*

### They revealed the secrets of exotic matter

This year’s Laureates opened the door on an unknown world where matter can assume strange states. They have used advanced mathematical methods to study unusual phases, or states, of matter, such as superconductors, superfluids or thin magnetic films. Thanks to their pioneering work, the hunt is now on for new and exotic phases of matter. Many people are hopeful of future applications in both materials science and electronics.

to understand the properties of chains of small magnets found in some materials.

We now know of many topological phases, not only in thin layers and threads, but also in ordinary three-dimensional materials. Over the last decade, this area has boosted frontline research in condensed matter physics, not least because of the hope that topological materials could be used in new generations of electronics and superconductors, or in future quantum computers. Current

# Tour of topological physics



- The 2016 Nobel prize
- The Quantum Hall effect



- Haldane model
- Topological Insulators



- Unconventional superconductivity in  $\text{Sr}_2\text{RuO}_4$



- Kerr effect in  $\text{Sr}_2\text{RuO}_4$



- Superfluid angular momentum and orbital magnetization of  $\text{Sr}_2\text{RuO}_4$

# 🌿 Thouless, Haldane and Kosterlitz

- Kosterlitz Thouless 1973 paper  
Birmingham 2d superfluids and 2d melting
- Haldane topological aspects of quantum fields (eg 1+1d  $S=1$  antiferromagnet)
- Thouless classification of topological states



# 🌟 Quantum Hall effect, 1980

- von Klitzing Nobel prize 1985

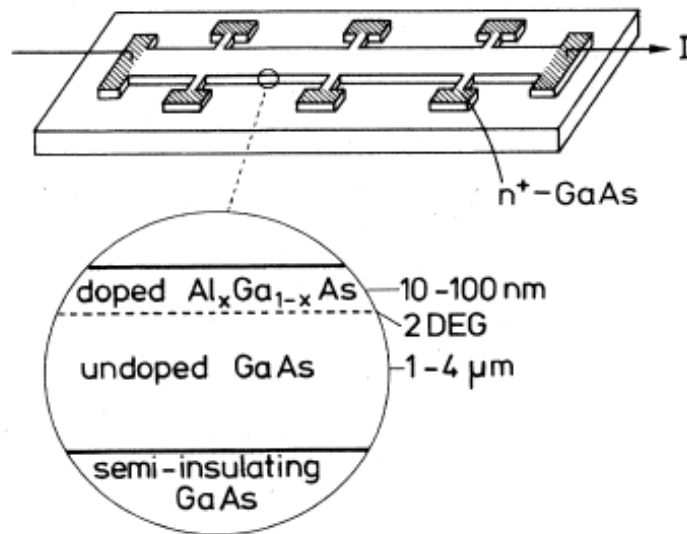


FIG. 3. Typical shape and cross section of a GaAs-Al<sub>x</sub>Ga<sub>1-x</sub>As heterostructure used for Hall-effect measurements.

# Quantum Hall effect

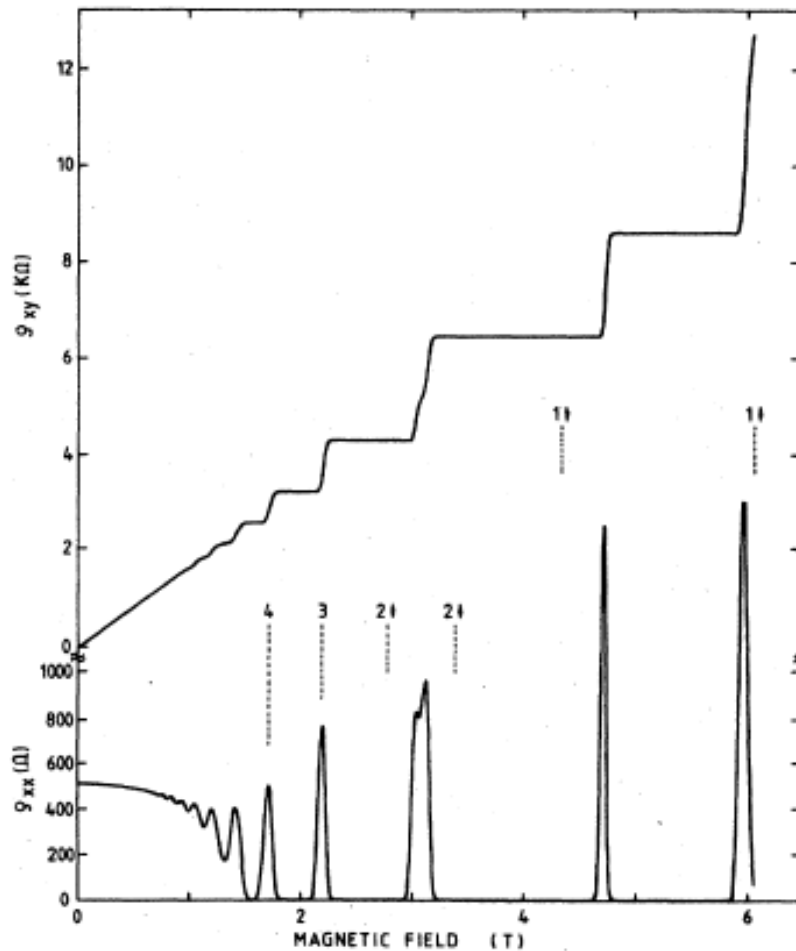


FIG. 14. Experimental curves for the Hall resistance  $R_H = \rho_{xy}$  and the resistivity  $\rho_{xx} \sim R_x$  of a heterostructure as a function of the magnetic field at a fixed carrier density corresponding to a

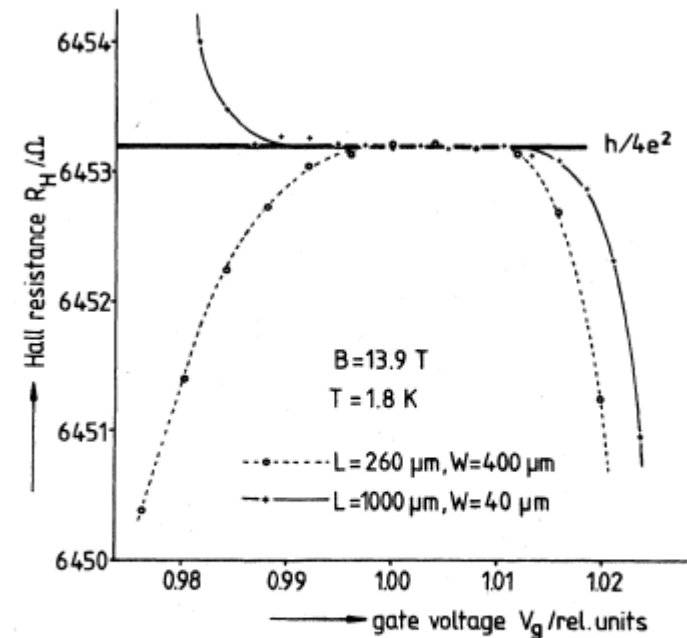


FIG. 10. Hall resistance  $R_H$  for two different samples with different aspect ratios  $L/W$  as a function of the gate voltage ( $B = 13.9$  T).

# Conductance in solids

- The conductance relates current density to electric field
- We can distinguish longitudinal and Hall conductance
- Both form elements of the conductivity tensor
- There is a natural unit of conductance,  $e^2/h$
- The QHE is so precise that it can be used for precision measurements of this ratio of the fundamental constants

$$\mathbf{j} = \boldsymbol{\sigma} \mathbf{E}$$

$$\begin{pmatrix} j_x \\ j_y \end{pmatrix} = \begin{pmatrix} \sigma_{xx} & \sigma_{xy} \\ \sigma_{yx} & \sigma_{yy} \end{pmatrix} \begin{pmatrix} E_x \\ E_y \end{pmatrix}$$

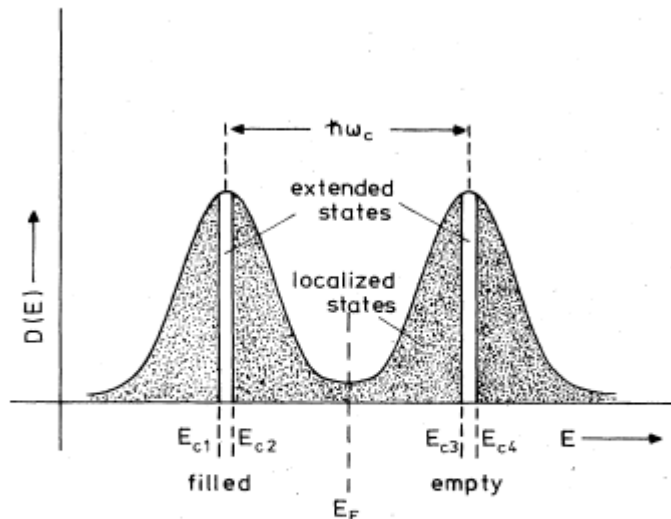
$$\sigma_{xy} = N \frac{e^2}{h}$$



# 🌟 Topology in QHE

Why is the Hall conductance so accurate in a disordered material?

Disorder makes almost all states non-conducting  
The exception are topological **edge states**



RB Laughlin, Nobel prize 1998  
(for the fractional QHE)

FIG. 6. Model for the broadened density of states of a 2DEG in a strong magnetic field. Mobility edges close to the center of the Landau levels separate extended states from localized states.



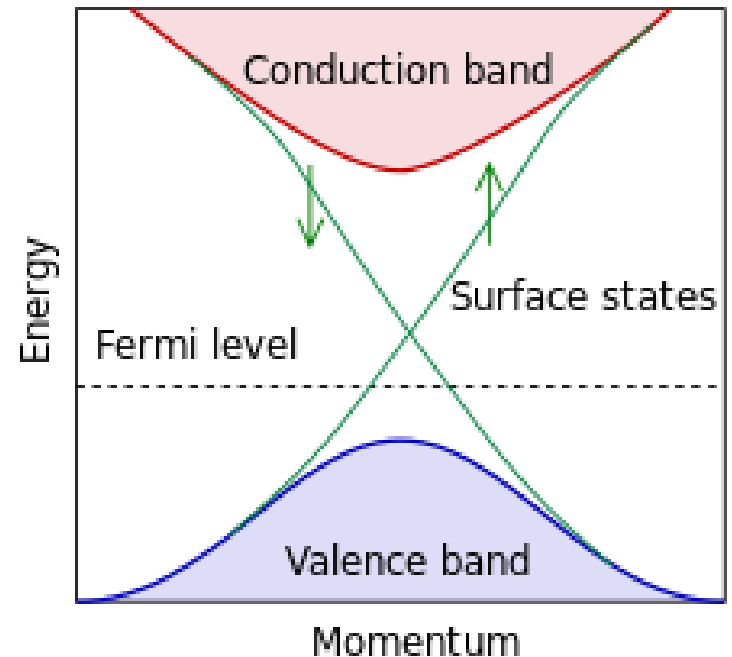
# 🌿 Its all at the edge

- Consider a crude analogy walking in a landscape
- Follow a fixed height (energy) contour and we always end up back where we started from just walking around the same contour.
- Eg in an island there is always one contour which goes around the edge at fixed height
- Electrons in the QHE do the same, all the current flows around the edge?

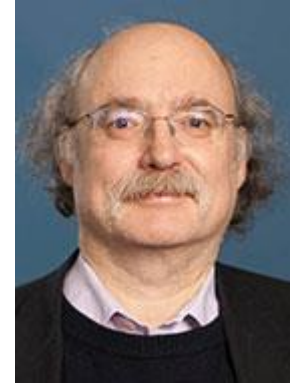


# 🌿 Topological insulators

- Any insulator may have surface states
- But a topological insulator must have edge states
- These conduct without dissipation (no scattering)
- Chiral, Weyl fermions



# 🌿 The Haldane model 1988



- A ‘toy’ model of graphene with artificial second neighbour hopping
- It can be an insulator
- with Quantized Hall conductance (without external magnetic fields)
- All current carried in edge states

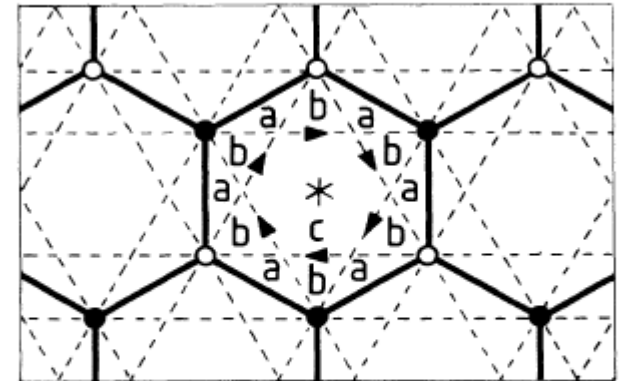


FIG. 1. The honeycomb-net model (“2D graphite”) showing nearest-neighbor bonds (solid lines) and second-neighbor bonds (dashed lines). Open and solid points, respectively, mark the vertices and midpoints of the nearest-neighbor bonds.

$$\sigma_{xy} = N e^2/h, \quad N = \text{Chern number}$$

# Topological Superconductivity?

- Spin-triplet superconductivity and orbital magnetism in  $\text{Sr}_2\text{RuO}_4$
- Superconducting Kerr effect and Berry phases in multiband superconductors



# Collaborators

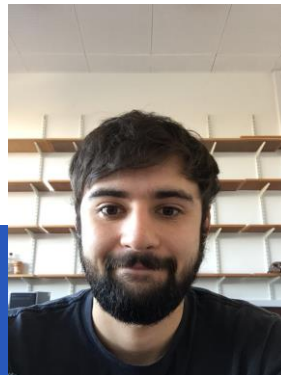
- Thanks to my collaborators!

Karol Wysokinski  
(Lublin)

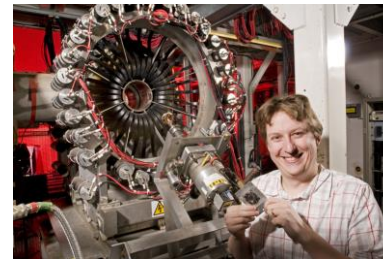


Jorge Quintanilla  
(ISIS/ Kent)

Gregorz Litak  
(Lublin)



Adrian Hillier (ISIS)



Joshua Robbins



Balazs Gyorffy (1938-2012)

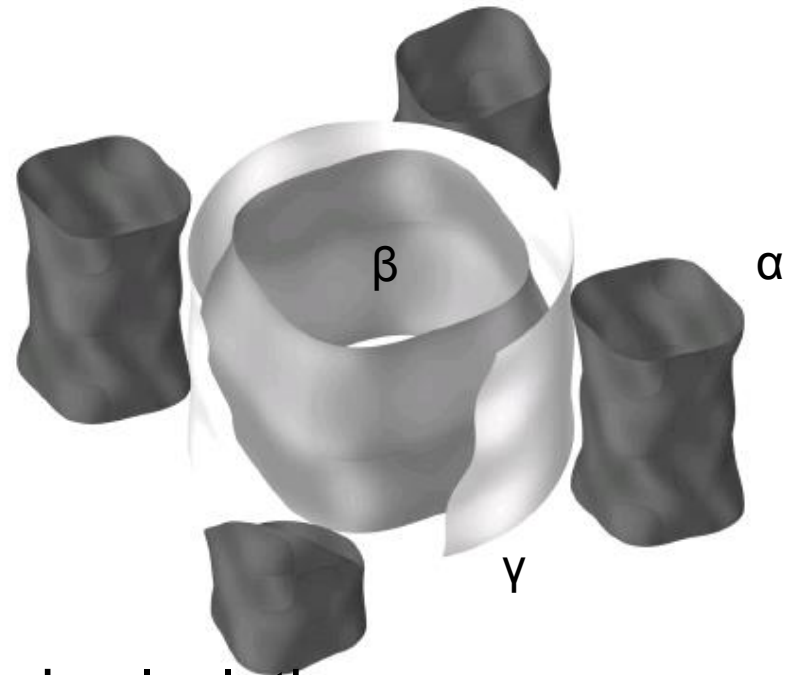


Martin Gradhand



# 🌿 The Fermi surface in $\text{Sr}_2\text{RuO}_4$

There are three cylindrical Fermi surface sheets, measured with great accuracy by Bergman and Mackenzie



These agree well with LDA band calculations, and are derived from the Ru 4d  $T_{2g}$  multiplet of d states  $|xz\rangle$ ,  $|yz\rangle$  (giving  $\alpha\beta$ ) and  $|x^2-y^2\rangle$  (giving  $\gamma$ )



# 🌟 A solid state analogue of $^3\text{He-A}$ ?

TABLE I: Irreducible representations of even and odd parity in a tetragonal crystal. The symbols  $X, Y, Z$  represent any functions transforming as  $x, y$  and  $z$  under crystal point group operations, while  $I$  represents any function which is invariant under all point group symmetries.

Rep.	symmetry	Rep.	symmetry
$A_{1g}$	$I$	$A_{1u}$	$XYZ(X^2 - Y^2)$
$A_{2g}$	$XY(X^2 - Y^2)$	$A_{2u}$	$Z$
$B_{1g}$	$X^2 - Y^2$	$B_{1u}$	$XYZ$
$B_{2g}$	$XY$	$B_{2u}$	$Z(X^2 - Y^2)$
$E_g$	$\{XZ, YZ\}$	$E_u$	$\{X, Y\}$

In a tetragonal crystal group theory allows a set of d-wave pairing states or p-wave states similar to  $^3\text{He}$  (Annett Adv. Phys 1990)

P-wave triplet states based on the  $E_u$  irreducible representation include an analogue of the ABM phase

$$\mathbf{d}_k = (\sin(k_x) + i \sin(k_y)) \mathbf{e}_z$$

This corresponds to the crystal analogue of  $L_z=1, S_z=0$  ( $|\uparrow\downarrow + \downarrow\uparrow\rangle$ ) triplet pairing



# A model chiral pairing state

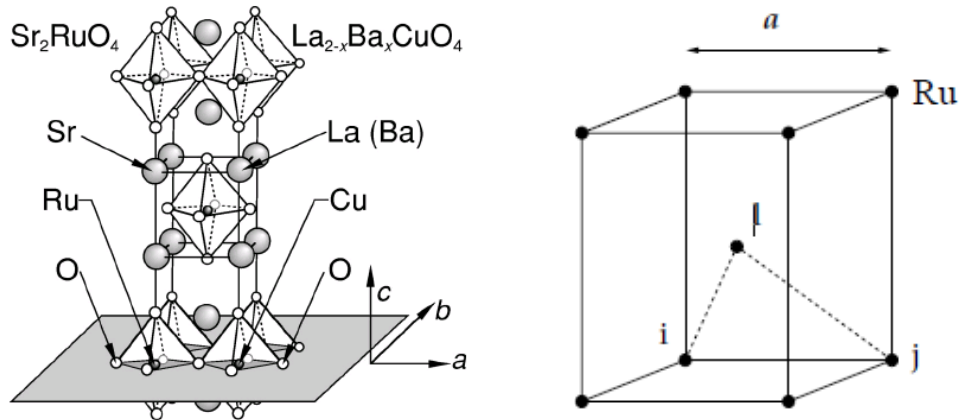


FIG. 1. The layered perovskite structure common to ruthenate and cuprate superconductors.

$\text{Sr}_2\text{RuO}_4$  is a body-centred tetragonal crystal. Symmetry analysis (JFA Adv. Phys. 1990) of possible superconducting states shows only 2 possible time reversal pairing states: d-wave singlet or p-wave triplet.

In order to match experimental specific heat data showing a line node we include interlayer interactions in our model, leading to horizontal line nodes on  $\alpha\beta$  sheets

TABLE I: Irreducible representations of even and odd parity in a tetragonal crystal. The symbols  $X, Y, Z$  represent any functions transforming as  $x, y$  and  $z$  under crystal point group operations, while  $I$  represents any function which is invariant under all point group symmetries.

Rep.	symmetry	Rep.	symmetry
$A_{1g}$	$I$	$A_{1u}$	$XYZ(X^2 - Y^2)$
$A_{2g}$	$XY(X^2 - Y^2)$	$A_{2u}$	$Z$
$B_{1g}$	$X^2 - Y^2$	$B_{1u}$	$XYZ$
$B_{2g}$	$XY$	$B_{2u}$	$Z(X^2 - Y^2)$
$E_g$	$\{XZ, YZ\}$	$E_u$	$\{X, Y\}$

TABLE III: Basis functions  $\gamma_i^\Gamma(\mathbf{k})$  for the odd parity irreducible representations of body-centred tetragonal crystals.

Rep.	in-plane	inter-plane
$A_{1u}$	-	-
$A_{2u}$	-	$\cos \frac{k_x}{2} \cos \frac{k_y}{2} \sin \frac{k_z c}{2}$
$B_{1u}$	-	$\sin \frac{k_x}{2} \sin \frac{k_y}{2} \sin \frac{k_z c}{2}$
$B_{2u}$	-	-
$E_u$	$\sin k_x$	$\sin \frac{k_x}{2} \cos \frac{k_y}{2} \cos \frac{k_z c}{2}$
	$\sin k_y$	$\cos \frac{k_x}{2} \sin \frac{k_y}{2} \cos \frac{k_z c}{2}$

$a$



Time reversal symmetry breaking  
by superconductivity  
in  $\text{Sr}_2\text{RuO}_4$



# 🌟 Spontaneous time reversal symmetry breaking in $\text{Sr}_2\text{RuO}_4$

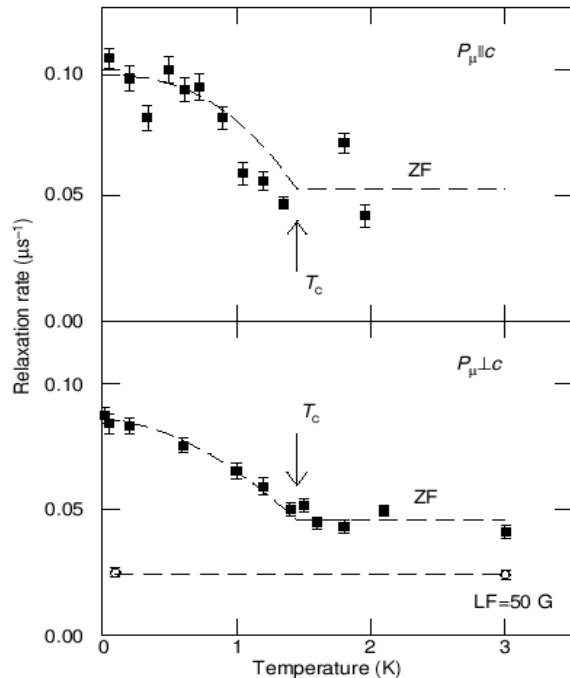


**Figure 2** Zero-field (ZF) relaxation rate  $\Lambda$  for the initial muon spin polarization  $\parallel c$  (top) and  $\perp c$  (bottom).  $T_c$  from a.c.-susceptibility indicated by arrows. Circles in bottom figure give relaxation rate in  $B_{LF} = 50 \text{ G} \perp c$ . Curves are guides to the eye.

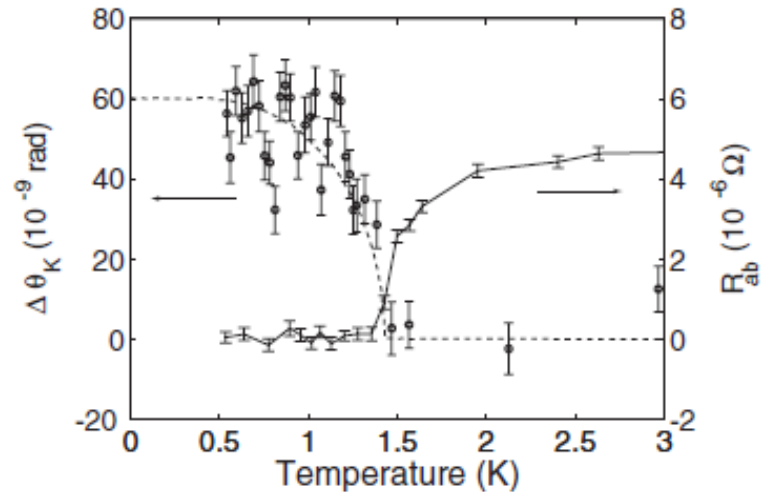


**FIG. 2.** Zero-field (earth field) measurement of Kerr effect (O) and  $ab$ -plane electrical resistance (dotted line). Dashed curve is a fit to a BCS gap temperature dependence.

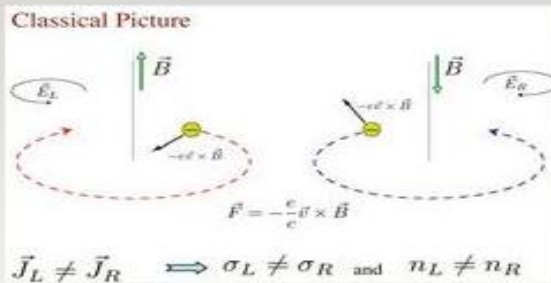
Optical Kerr effect,  
Xia et al, PRL 2006

Muon spin rotation, Luke et al Nature 1988

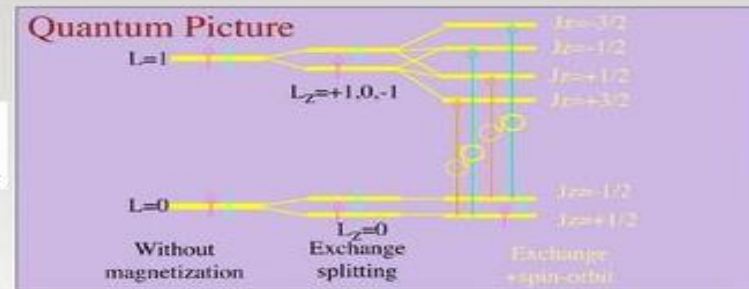
# 🔥 The polar Kerr effect

Dichroism: different refractive indices for left and right circular polarized light, leads to rotation of the plane of polarization of reflected light in magnetic materials

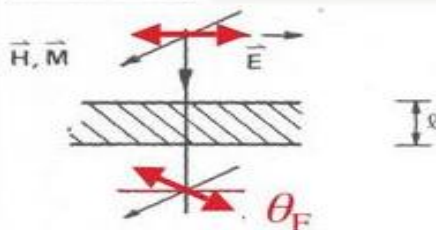
## Magneto-Optical-like Measurements!



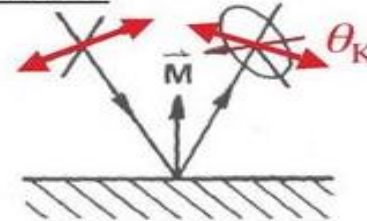
$$n_R \neq n_L$$



### Faraday Effect:



### (Polar) Kerr Effect:



# 🌟 The Kerr angle and Hall conductance

$$\theta_K = \frac{4\pi}{\omega} \operatorname{Im} \frac{\sigma_{xy}(\omega)}{n(n^2 - 1)}$$

$$\omega > \omega_{ab} \quad \theta_K = \frac{4\pi\omega^2 \operatorname{Im}\sigma_{xy}(\omega)}{\sqrt{\epsilon_\infty\omega^2 - \omega_{ab}^2} [(\epsilon_\infty - 1)\omega^2 - \omega_{ab}^2]}$$

$$\omega < \omega_{ab} \quad \theta_K = -\frac{4\pi\omega^2 \operatorname{Re}\sigma_{xy}(\omega)}{\sqrt{\omega_{ab}^2 - \epsilon_\infty\omega^2} [(\epsilon_\infty - 1)\omega^2 - \omega_{ab}^2]}$$

$\omega_{ab}$  - plasma frequency



# Kerr effect in superconductors

- In one band models of chiral superconductors there have been many attempts to obtain the Kerr effect, eg
- Yip and Sauls (1992)
- Li and Joynt (1991)
- Yakovenko 2007
- Minnev 2007
- However the analysis of one band models is now believed to give zero signal, except as a result of impurity scattering (Goryo 2008, Lutchyn 2009)
- But  $\text{Sr}_2\text{RuO}_4$  is very clean, and so this seems unlikely as an explanation of the experiments.



# Dichroism from multiband chiral superconductivity

- In 2012 two papers proposed that a non-zero Kerr signal arises from multiband/inter-orbital effects, even in the clean limit
- **Edward Taylor, Catherine Kallin** *Phys. Rev. Lett.* **108**, 157001 (2012): two – band, two dimensional model fitted to DFT band structure.
- **KI Wysokinski, J. F. Annett, B. L. Gyorffy** *PRL* **108**, 077004 (2012): three – band, three dimensional model fitted to experimental Fermi surface close to EF. Dichroic signal from interband (interorbital) processes.
- These two papers had a similar approach and gave similar magnitude effect at the experimental frequencies, but the results differed considerably in detail.
- V.P.Mineev (*J.Phys. Soc. Jpn.* **81**,093703 (2012)) argued against multi-orbital scenario altogether using symmetry analysis



# Kerr Effect in $\text{Sr}_2\text{RuO}_4$

the electromagnetic power absorption  $P(\omega, \epsilon)$  for light of left and right circular polarizations,  $\epsilon_L$  and  $\epsilon_R$ , respectively,

$$\text{Im}[\sigma_{xy}(\omega)] = \frac{1}{VE_0^2} [P(\omega, \epsilon_L) - P(\omega, \epsilon_R)]. \quad (1)$$

Here  $V$  is the sample volume,  $E_0$  is the electric field strength of the light, and  $\epsilon_{L/R} = (1, \pm i, 0)/\sqrt{2}$ . Within the BdG formalism the absorption spectrum can be calculated directly in terms of the dipole matrix elements

$$P(\omega, \epsilon) = \frac{\pi^2 e^2 E_0^2}{2\omega} \sum_{N, N', \mathbf{k}} f(E_N(\mathbf{k})) [1 - f(E_{N'}(\mathbf{k}))] \\ \times |\langle N' \mathbf{k} | \hat{H}_I(\epsilon) | N \mathbf{k} \rangle|^2 \delta(E_{N'}(\mathbf{k}) - E_N(\mathbf{k}) - \hbar\omega) \quad (2)$$

where

$$|N \mathbf{k}\rangle = \begin{pmatrix} u_N(\mathbf{k}) \\ v_N(\mathbf{k}) \end{pmatrix} \quad (3)$$

is the  $N$ th eigenvector of the BdG equation at wave vector  $\mathbf{k}$ ,

$$\begin{pmatrix} \hat{H}_0(\mathbf{k}) & \hat{\Delta}(\mathbf{k}) \\ \hat{\Delta}(\mathbf{k})^\dagger & -\hat{H}_0(\mathbf{k})^* \end{pmatrix} \begin{pmatrix} u_N(\mathbf{k}) \\ v_N(\mathbf{k}) \end{pmatrix} = E_N \begin{pmatrix} u_N(\mathbf{k}) \\ v_N(\mathbf{k}) \end{pmatrix}. \quad (4)$$

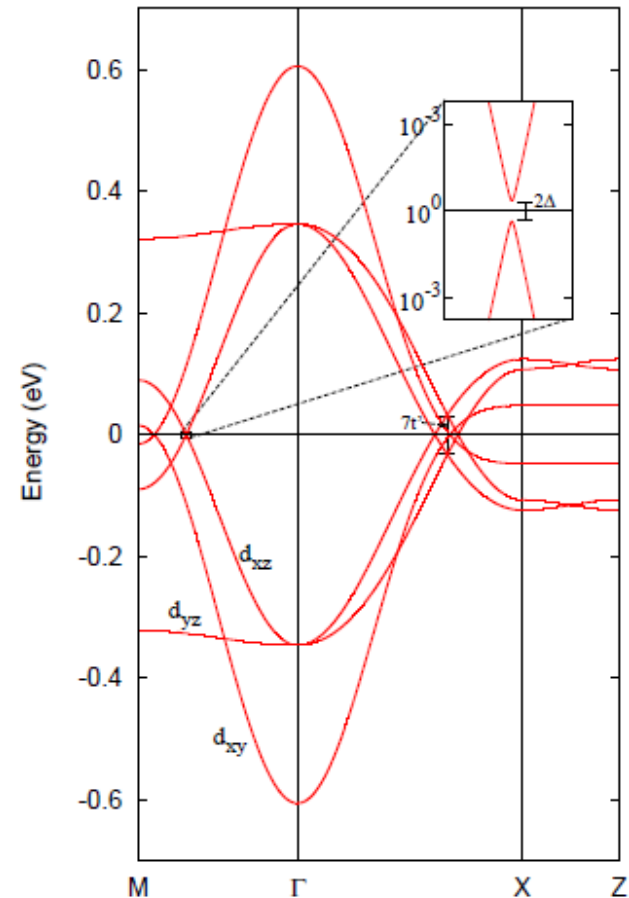
Method of: K. Capelle,  
E.K.U. Gross and B.L.  
Gyorffy, Phys. Rev.  
Lett. **78** 3753 (1997).

The dichroism is calculated in terms of optical absorption spectra, evaluated relative to the chiral superconducting state

Here we have INTERBAND transitions (non-diagonal in orbital space) which are not present in single band approach

# 🌟 Optical transitions in the 3 band model below $T_c$

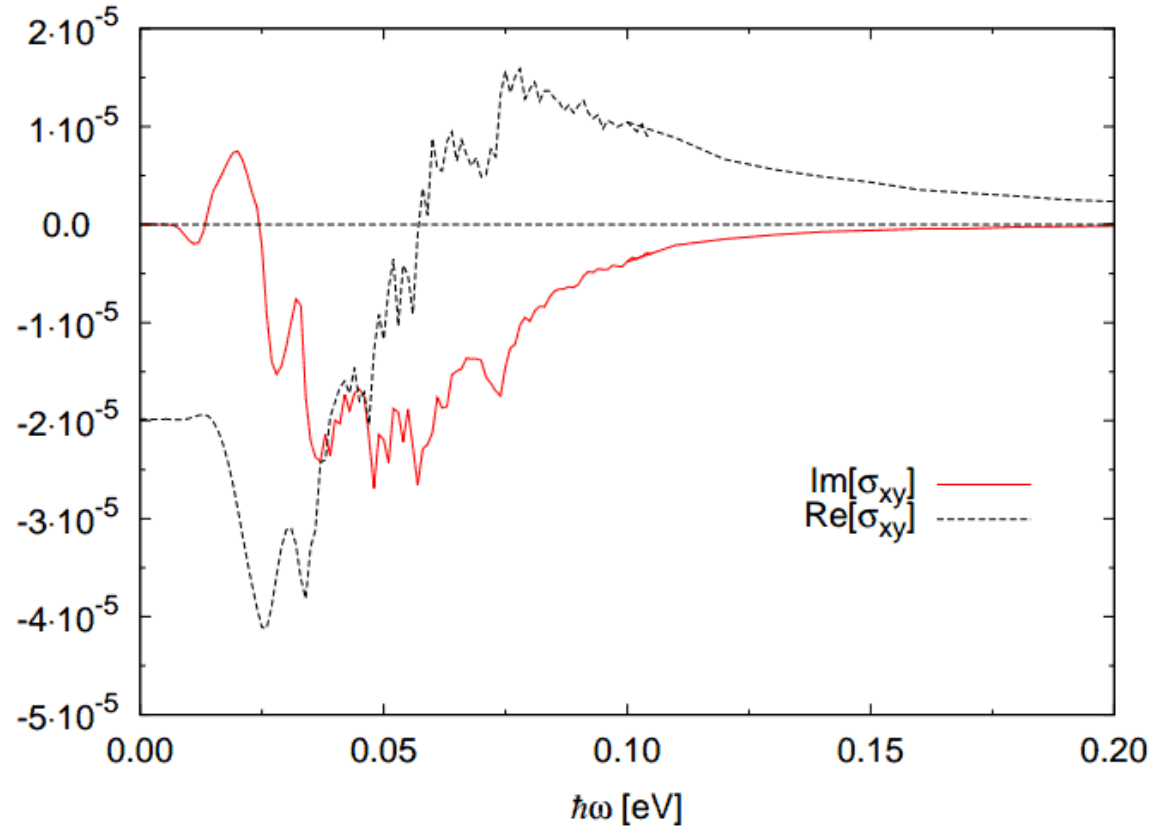
- The quasiparticle states come in positive and negative energy bands, with a small gap at zero.
- A variety of optical transitions interband can be possible
- The  $d_{xy}$  bands are decoupled, but  $d_{xz}$  to  $d_{yz}$  transitions occur in some parts of the zone



# 🔥 Calculated Hall spectrum (Gradhand et al, PRB 2013)

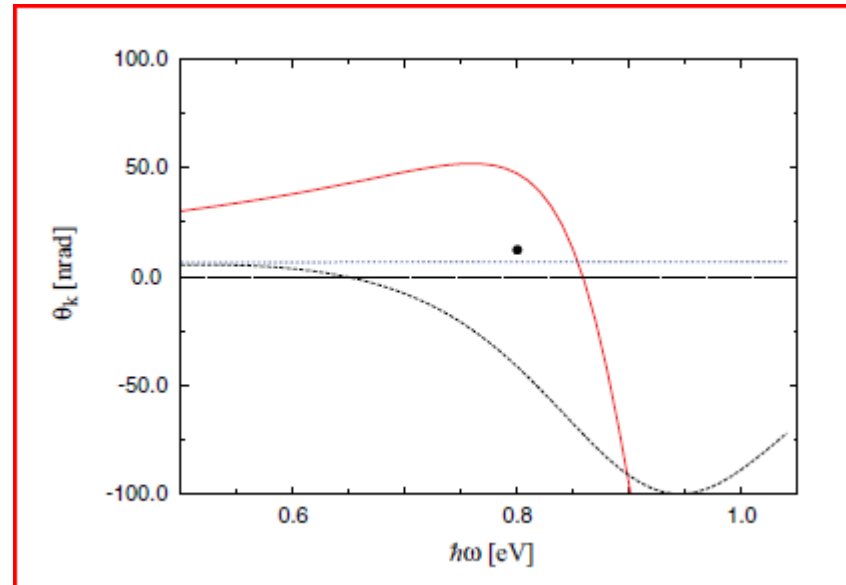
Imaginary part is zero at low frequencies, threshold at interband energy (not gap energy)

Differences from Taylor and Kallin appear mainly from different band-structures used (dHvA fit vs DFT, bandwidths differ by  $m^*/m \approx 2-3$ )



# 🌟 Estimated Hall angle at 0.6eV

- At the single experimental frequency of 0.6eV our spectrum is dependent on models of bulk plasma frequency and damping
- Estimates are consistent with experimental magnitude of 80-90nRad



- Figure shows three estimated values based on two models of plasma response

# Berry phase approach to orbital magnetism and Kerr effect in multiband superconductors



# Berry curvature of Bloch electrons

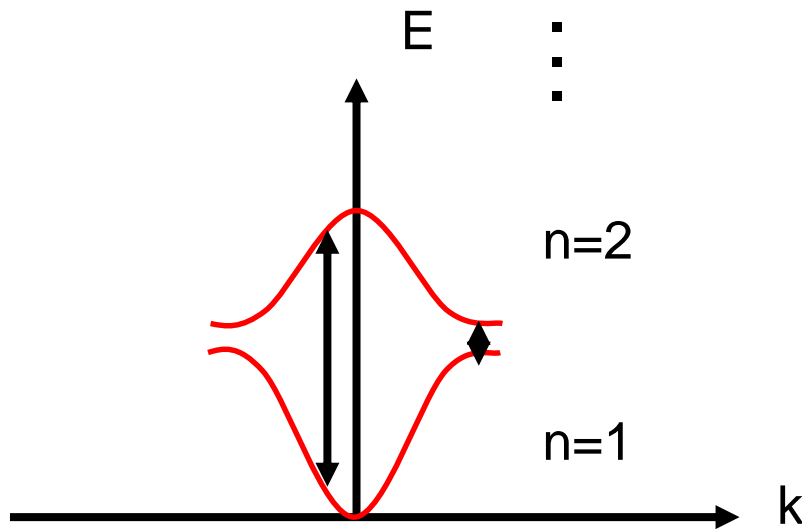
Bloch function:  $\Psi_{n\mathbf{k}}(\mathbf{r}) = e^{i\mathbf{k}\cdot\mathbf{r}} u_{n\mathbf{k}}(\mathbf{r})$

Parameter-dependent  
Hamiltonian:  $H_{\mathbf{k}} u_{n\mathbf{k}}(\mathbf{r}) = \mathcal{E}_n(\mathbf{k}) u_{n\mathbf{k}}(\mathbf{r})$

Berry curvature:  $\Omega_n(\mathbf{k}) = \nabla_{\mathbf{k}} \times \mathcal{A}_n(\mathbf{k})$

Berry connection:  $\mathcal{A}_n(\mathbf{k}) = i \int_{\omega} u_{n\mathbf{k}}^{\dagger}(\mathbf{r}) \nabla_{\mathbf{k}} u_{n\mathbf{k}}(\mathbf{r}) d\mathbf{r}$

# Berry curvature of Bloch electrons



Berry curvature

$$\Omega_n(\mathbf{k}) = i(\nabla_{\mathbf{k}} u_{n\mathbf{k}}(\mathbf{r}), \times \nabla_{\mathbf{k}} u_{n\mathbf{k}}(\mathbf{r}))$$

$$H_{\mathbf{k}} u_{n\mathbf{k}}(\mathbf{r}) = \mathcal{E}_n(\mathbf{k}) u_{n\mathbf{k}}(\mathbf{r})$$

$$\Omega_n(\mathbf{k}) = i \sum_{m \neq n} \frac{(u_{n\mathbf{k}}(\mathbf{r}), \nabla_{\mathbf{k}} H_{\mathbf{k}} u_{m\mathbf{k}}(\mathbf{r})) \times (u_{m\mathbf{k}}(\mathbf{r}), \nabla_{\mathbf{k}} H_{\mathbf{k}} u_{n\mathbf{k}}(\mathbf{r}))}{(\mathcal{E}_n - \mathcal{E}_m)^2}$$



# 🌿 Hall conductance sum rules and Berry phase

- For the normal state the following sum rule is obeyed by the Hall conductance

Kramers–Kronig transformation. It was shown by Souza and Vanderbilt that in this case the relation [15]

$$\int_0^{\infty} d\omega \frac{\text{Im}(\sigma_{xy}(\omega))}{\omega} = -\frac{e^2\pi}{2h} \sum_n \int \frac{d^3k}{(2\pi)^3} \Omega_n^z(\mathbf{k}) f(E_n(\mathbf{k}))$$

We are now consider the extension of this work to the superconducting case.





**IOP** Publishing

Journal of Physics: Condensed Matter

J. Phys.: Condens. Matter **26** (2014) 274205 (7pp)

[doi:10.1088/0953-8984/26/27/274205](https://doi.org/10.1088/0953-8984/26/27/274205)

# The Berry curvature of the Bogoliubov quasiparticle Bloch states in the unconventional superconductor $\text{Sr}_2\text{RuO}_4$

Martin Gradhand and James F Annett

H H Wills Physics Laboratory, University of Bristol, Tyndall Avenue, BS8 1TL, UK



University of  
**BRISTOL**



# Berry phases in the Bogoliubov de Gennes Hamiltonian

- The Bogoliubov de Gennes Hamiltonian obeys Bloch's theorem
- The quasiparticle wave functions are written in terms of a plane wave,  $\mathbf{k}$ , and a part  $(u_{\mathbf{k}}(\mathbf{r}), v_{\mathbf{k}}(\mathbf{r}))$  with electron/hole terms which is periodic in space
- In this basis we have a  $\mathbf{k}$  dependent Hamiltonian,

crystal we can separate the Bloch phase factor from the lattice periodic part of the wavefunction as in the normal state [13]  $\langle \mathbf{r} | \Psi_{n\mathbf{k}} \rangle = e^{i\mathbf{k}\mathbf{r}} (u_{n\mathbf{k}}(\mathbf{r}), v_{n\mathbf{k}}(\mathbf{r}))^T$  and retrieve an equation for the periodic wavefunction within one unit cell (UC) [13]

$$\begin{pmatrix} \hat{H}_{\mathbf{k}}(\mathbf{r}) & \hat{\Delta}(\mathbf{r}) \\ \hat{\Delta}^\dagger(\mathbf{r}) & -\hat{H}_{-\mathbf{k}}^*(\mathbf{r}) \end{pmatrix} \begin{pmatrix} u_{n\mathbf{k}}(\mathbf{r}) \\ v_{n\mathbf{k}}(\mathbf{r}) \end{pmatrix} = E_{n\mathbf{k}} \begin{pmatrix} u_{n\mathbf{k}}(\mathbf{r}) \\ v_{n\mathbf{k}}(\mathbf{r}) \end{pmatrix}. \quad (2)$$

Here, the  $\mathbf{k}$ -dependent lattice periodic normal state Hamiltonian  $\hat{H}_{\mathbf{k}} = e^{-i\mathbf{k}\mathbf{r}} \hat{H}(\mathbf{r}) e^{i\mathbf{k}\mathbf{r}}$  appears on the diagonals and the  $\mathbf{k}$  independent local gap function  $\hat{\Delta}(\mathbf{r})$  is connecting electron and hole like states on the off-diagonal part of the operator.



# 🌿 Berry phases in the BdeG Hamiltonian

- The Berry phases can be defined as usual, leading to the Berry curvature

the following. The formal definition of the Berry curvature of Bloch states is [1–3, 14]

$$\begin{aligned}\Omega_n(\mathbf{k}) &= i\nabla_{\mathbf{k}} \times \int_{\text{UC}} d^3r \Phi_{n\mathbf{k}}^*(\mathbf{r}) \nabla_{\mathbf{k}} \Phi_{n\mathbf{k}}(\mathbf{r}) \\ &= i\nabla_{\mathbf{k}} \times (\Phi_{n\mathbf{k}}(\mathbf{r}), \nabla_{\mathbf{k}} \Phi_{n\mathbf{k}}(\mathbf{r})),\end{aligned}\quad (3)$$

where  $(\cdot, \cdot)$  is a shorthand notation for the inner product of the periodic part of the Bloch function defined as the real



# 🌟 Hall conductance sum rule

- We can then prove the following relation for the Hall conductance in the superconducting state

$$\sum_{nk} \Omega_n(\mathbf{k}) f(E_{nk}) = \frac{\pi e^2}{2V \hbar^2} \sum_{n,m,\mathbf{k}} f(E_{nk}) [1 - f(E_{mk})] \times \frac{\text{Im}[\langle nk | \nabla_{\mathbf{k}} \hat{M}_{\mathbf{k}} | m\mathbf{k} \rangle \times \langle m\mathbf{k} | \nabla_{\mathbf{k}} \hat{M}_{\mathbf{k}} | n\mathbf{k} \rangle]}{(E_m(\mathbf{k}) - E_n(\mathbf{k}))^2}. \quad (13)$$

This yields immediately the desired Hall sum rule relating the integral over the optical conductivity to the sum over all occupied bands of the Berry curvature

$$\int_0^\infty d\omega \frac{\text{Im}(\sigma_{xy}(\omega))}{\omega} = -\frac{\pi e^2}{2\hbar} \sum_n \int \frac{d^3k}{(2\pi)^3} \Omega_n^z(\mathbf{k}) f(E_{nk}), \quad (14)$$

$$\hat{M}_{\mathbf{k}}(\mathbf{r}) = \begin{pmatrix} \hat{H}_{\mathbf{k}}(\mathbf{r}) & \hat{\Delta}(\mathbf{r}) \\ \hat{\Delta}^\dagger(\mathbf{r}) & -\hat{H}_{-\mathbf{k}}^*(\mathbf{r}) \end{pmatrix}.$$

# 🔥 Zero-frequency real part of Hall conductance

- Using Kramers-Kronig this integral also gives the real Hall conductance at zero frequency

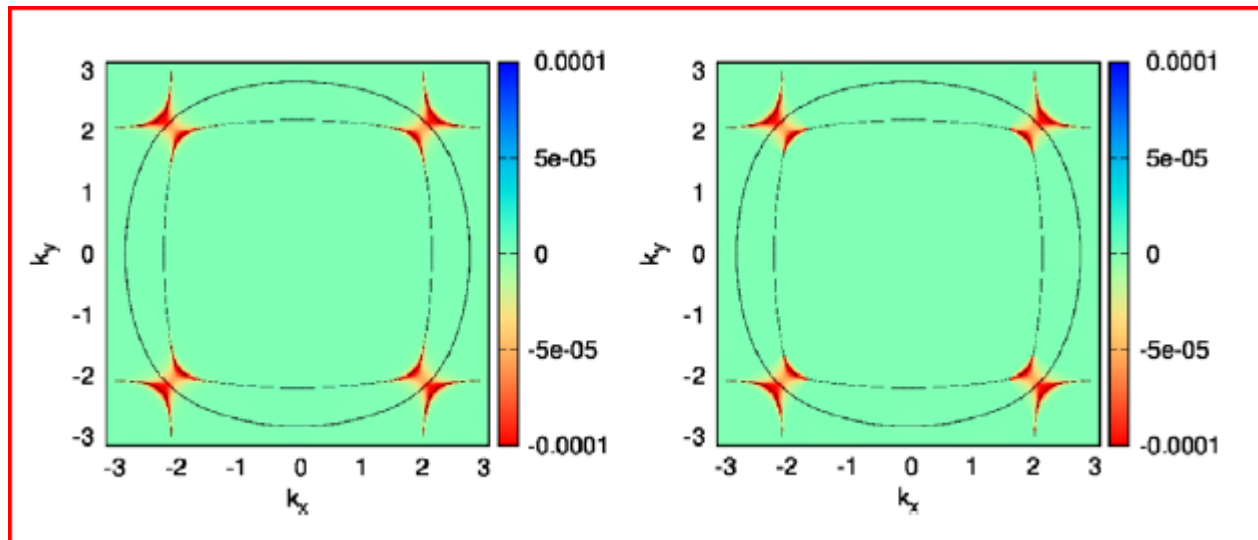
out that due to Kramers–Kronig transformation the integral of equation (14) is related to the zero frequency real part of the optical conductivity and we can connect this quantity via

$$\text{Re}(\sigma_{xy}(\omega = 0)) = -\frac{e^2}{\hbar} \sum_n \int \frac{d^3k}{(2\pi)^3} \Omega_n^z(\mathbf{k}) f(E_{n\mathbf{k}}), \quad (15)$$



# 🌿 K-dependence of Berry curvatures for $\text{Sr}_2\text{RuO}_4$

- We can compare the direct calculation of contributions to the Hall conductance sum rule in k-space (left) with the corresponding Berry curvatures (right) in our model



# Orbital Magnetism in Sr<sub>2</sub>RuO<sub>4</sub>?

- If the superconducting state breaks 'time reversal' symmetry it is effectively magnetic
- Is there a magnetic moment in the superconducting state?
- If so, how does it relate to the Kerr effect?



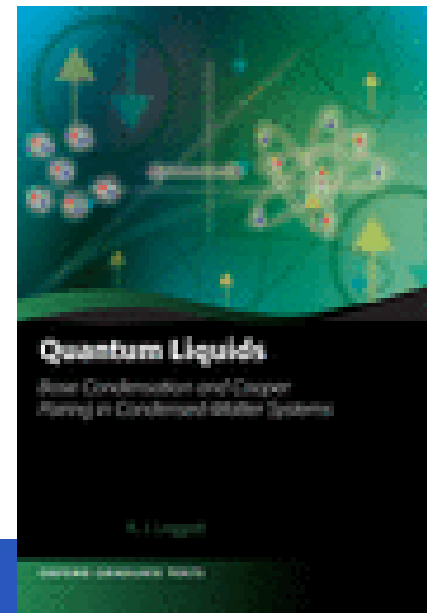
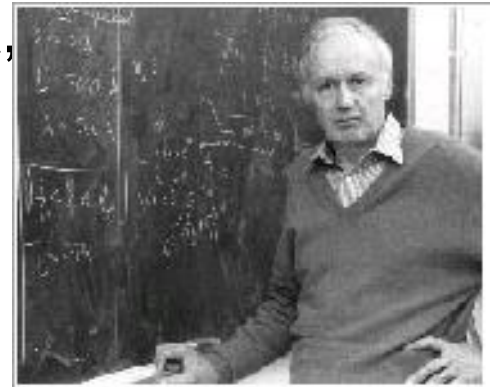
# 🌟 “Angular momentum” of $^3\text{He-A}$

- Tony Leggett discusses this in appendix 6A, of his book “*Quantum Liquids: Bose Condensation and Cooper Pairing in Condensed Matter Systems*”
- He notes that the trial state

$$\Psi_N = \left( \sum_k |c_k| e^{i\phi_k} a_k^+ a_{-k}^+ \right)^{N/2} |vac\rangle$$

(dropping spin indices for clarity)

is an exact eigenstate of  $L_z$  with eigenvalue  $N\hbar/2$   
(ignoring subtleties about boundary conditions)



# “Angular momentum” of $^3\text{He-A}$

- But this result is independent of the superconductivity. It is true even if  $d_{\mathbf{k}}=0$ !
- The wave function corresponds to a BEC of  $N$  molecules, each in a  $l_z=\hbar/2$  internal state
- For a Fermi liquid we should write a different wave function, such as

$$\Psi_N = \left( \sum_{k>k_f} |c_k| e^{i\phi_k} a_k^+ a_{-k}^+ \right)^{N_+/2} \left( \sum_{k<k_f} |c_k| e^{-i\phi_k} a_{-k} a_k \right)^{N_-/2} |FS\rangle$$

- This is also an eigenvector of  $L_z$ , but now with eigenvalue  $L_z=0$  assuming particle hole symmetry!
- A finite value is only obtained as  $(N_+-N_-)\hbar/2$  if particle-hole-h symmetry is not exact, ie beyond weak coupling  $\Delta \ll E_f$



# The angular momentum paradox

- These results led to a 40 year long controversy of the correct definition of the orbital angular momentum in the chiral state of  $^3\text{He}$
- Probably the modern consensus is that there IS an orbital moment of  $N\hbar/2$ , and this is essentially entirely, due to a chiral edge state (M Stone)
- The existence of a bulk term arising from particle hole asymmetry is still not clearly established



# Orbital magnetism of $\text{Sr}_2\text{RuO}_4$

- The analog in a superconductor of orbital angular momentum is orbital MAGNETISM
- The intrinsic angular momentum of the condensate leads to orbital motion of charges, and hence magnetism
- Note that this is NOT magnetism due to electron spins, but due to their orbital motion.



# Simple calculation of the bulk orbital moment in $\text{Sr}_2\text{RuO}_4$

- The expectation of  $L_z$  within a single the d-shell for a single Ru ion is related to the single particle density matrix, and can be evaluated in the superconducting state by using the Bogoliubov transformation to the quasiparticle states

$$\langle \mathbf{L}_{\text{site}} \rangle = \langle \varphi_i | \mathbf{r} \times \mathbf{p} | \varphi_j \rangle n_{ij}$$

$$n_{ab}^{\sigma\sigma'} = \left\langle c_{a\sigma}^+ c_{b\sigma'} \right\rangle_{SC}$$

$$n_{mm'}^{\sigma\sigma} = \frac{1}{N_s} \sum_{\mathbf{k}} \sum_N [u_N^{*m\sigma}(\vec{k}) u_N^{m'\sigma}(\vec{k}) f(E_N(\vec{k})) + v_N^{m\sigma}(\vec{k}) v_N^{*m'\sigma}(\vec{k}) (1 - f(E_N(\vec{k})))].$$

The off diagonal contributions ( $m \neq m'$ ) are zero in the normal state and in non-chiral pairing states, but are non-zero in the chiral superconducting state

# 🔥 Spontaneous magnetism in $\text{Sr}_2\text{RuO}_4$

Unlike He-3  $\text{Sr}_2\text{RuO}_4$  has three sheets of Fermi surface corresponding to 3 Ru d orbitals.

We relate the orbital moment to orbital mixing induced by the chiral symmetry condensate

$$\langle L_z \rangle = n_{ab}^{\uparrow\uparrow} + n_{ab}^{\downarrow\downarrow} - (n_{ba}^{\uparrow\uparrow} + n_{ba}^{\downarrow\downarrow})$$

Where  $|a\rangle \equiv |xz\rangle$ ,  $|b\rangle \equiv |yz\rangle$  and  $n_{ab}^{\sigma\sigma'} = \langle c_{a\sigma}^+ c_{b\sigma'} \rangle_{SC}$

In the normal state these off-diagonal density matrix elements are zero, But in the chiral state they are non zero, of order  $|\Delta_0 N(0)|^2$ , and we obtain a small non-zero orbital moment per Ru atom, consistent with Kerr/MuSR experiments.

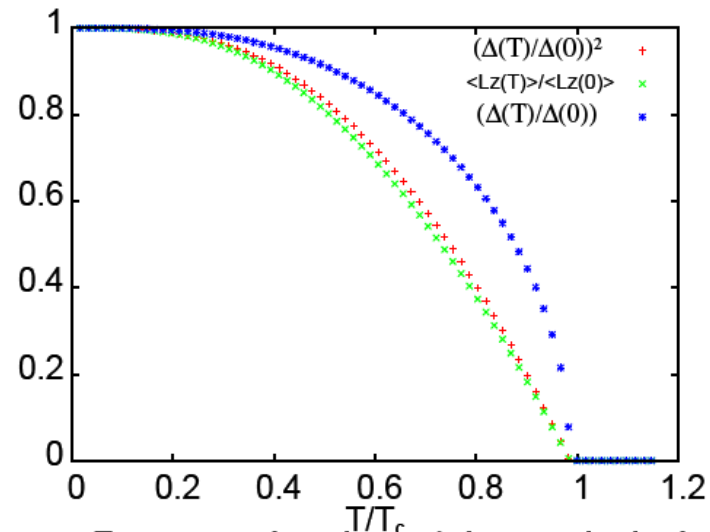


Figure 2. Temperature dependence of the normalised orbital moment  $\text{Sr}_2\text{RuO}_4$  in chiral state of  $\text{Sr}_2\text{RuO}_4$  calculated according to equation (15). Also shown are  $\Delta(T)/\Delta(0)$  and  $(\Delta(T)/\Delta(0))^2$ .

# 🔥 Orbital angular momentum in a crystal

- In a periodic crystal how to define an orbital magnetic moment?

$$\psi_{n\mathbf{k}}(\mathbf{r}) = \frac{1}{N_s^{1/2}} \sum_i e^{i\mathbf{k}\cdot\mathbf{R}_i} w_n(\mathbf{r} - \mathbf{R}_i)$$

Defining localized Wannier functions

the orbital angular momentum about site  $\mathbf{R}_0$  is:

$$\begin{aligned} \langle \hat{L}_z \rangle_0 &= \langle \Psi^N | \sum_{i=1,N} ([(\mathbf{r}_i - \mathbf{R}_0) \times \hat{\mathbf{p}}_i]_z) | \Psi^N \rangle \\ &= \sum_{n\mathbf{k}} \langle \psi_{n\mathbf{k}} | [(\mathbf{r} - \mathbf{R}_0) \times \hat{\mathbf{p}}]_z | \psi_{n\mathbf{k}} \rangle \\ &= \sum_{n\mathbf{k}} \frac{1}{N_s} \sum_{ij} e^{i\mathbf{k}\cdot(\mathbf{R}_j - \mathbf{R}_i)} \langle w_{ni} | [(\mathbf{r} - \mathbf{R}_0) \times \hat{\mathbf{p}}]_z | w_{nj} \rangle, \end{aligned}$$



# Orbital magnetism in insulators and metals

- Earlier we have used a ‘naïve’ picture of the orbital moment per atom. The theory of orbital magnetism in insulators was recently put on a more firm basis.

The proposal by Ceresoli, Thornhauser, Vanderbilt and Resta [9, 10] is that the following expression may be used for the orbital moment of a metal, insulator or Chern insulator

$$M = \frac{1}{2c(2\pi)^3} \text{Im} \sum_n \int_{\epsilon_{n\mathbf{k}} \leq \mu} d^3k \langle \nabla_{\mathbf{k}} u_{n\mathbf{k}} | \times (\hat{H}_{\mathbf{k}} + \epsilon_{n\mathbf{k}} - 2\mu) | \nabla_{\mathbf{k}} u_{n\mathbf{k}} \rangle \quad (18)$$

where  $u_{n\mathbf{k}}$  is the periodic part of the Bloch state  $\psi_{n\mathbf{k}}$ , the band energy is  $\epsilon_{n\mathbf{k}}$  and  $\hat{H}_{\mathbf{k}} = e^{-i\mathbf{k}\cdot\mathbf{r}} \hat{H} e^{i\mathbf{k}\cdot\mathbf{r}}$  where  $\hat{H}$  is the single particle crystal Hamiltonian.



# 🌿 Magnetization in $\text{Sr}_2\text{RuO}_4$ from Berry phases?

- Yes! Thanks to Martin Gradhand and Joshua Robbins
- Results similar to 'naive' approach
- Some Differences when spin-orbit coupling is introduced



# Topological Superconductivity

PHYSICAL REVIEW B 78, 195125 (2008)

## Classification of topological insulators and superconductors in three spatial dimensions

Andreas P. Schnyder,<sup>1</sup> Shinsei Ryu,<sup>1</sup> Akira Furusaki,<sup>2</sup> and Andreas W. W. Ludwig<sup>3</sup>

<sup>1</sup>*Kavli Institute for Theoretical Physics, University of California–Santa Barbara, Santa Barbara, California 93106, USA*

<sup>2</sup>*Condensed Matter Theory Laboratory, RIKEN, Wako, Saitama 351-0198, Japan*

<sup>3</sup>*Department of Physics, University of California–Santa Barbara, Santa Barbara, California 93106, USA*

(Received 11 April 2008; revised manuscript received 13 September 2008; published 26 November 2008)

We systematically study topological phases of insulators and superconductors (or superfluids) in three spatial dimensions. We find that there exist three-dimensional (3D) topologically nontrivial insulators or superconductors in five out of ten symmetry classes introduced in seminal work by Altland and Zirnbauer within the context of random matrix theory, more than a decade ago. One of these is the recently introduced  $Z_2$  topological insulator in the symplectic (or spin-orbit) symmetry class. We show that there exist precisely four more



# 🌟 Ten symmetry classes (taken from Schnyder et al PRB 2008)

**TABLE 1.** Ten symmetry classes of single particle Hamiltonians classified in terms of the presence or absence of time-reversal symmetry (TRS) and particle-hole symmetry (PHS), as well as sublattice (or “chiral”) symmetry (SLS) [17, 18, 19]. In the table, the absence of symmetries is denoted by “0”. The presence of these symmetries is denoted either by “+1” or “−1”, depending on whether the (anti-unitary) operator implementing the symmetry squares to “+1” or “−1”. For the first six entries of the table (which can be realized in non-superconducting systems) TRS = +1 when the SU(2) spin is integer and TRS = −1 when it is a half-integer. For the last four entries, the superconductor “Bogoliubov-de Gennes” (BdG) symmetry classes (denoted by the symbols D, C, DIII, and CI in “Cartan nomenclature”), it turns out that the Hamiltonian preserves SU(2) spin-1/2 rotation symmetry when PHS=−1 whilst it does not preserve SU(2) when PHS=+1. The column entitled “Hamiltonian” lists the spaces to which the quantum mechanical time-evolution operators of each symmetry class belong (see section B). The column entitled “NLSM (ferm. replicas)” lists the “target spaces” of Non-Linear Sigma Model field theories describing Anderson localization physics in each symmetry class (see section B).

System	Cartan nomenclature	TRS	PHS	SLS	Hamiltonian	NLSM (ferm. replicas)
standard (Wigner-Dyson)	A (unitary)	0	0	0	$U(N)$	$U(2n)/U(n) \times U(n)$
	AI (orthogonal)	+1	0	0	$U(N)/O(N)$	$Sp(2n)/Sp(n) \times Sp(n)$
	AII (symplectic)	−1	0	0	$U(2N)/Sp(2N)$	$O(2n)/O(n) \times O(n)$
chiral (sublattice)	AIII (chiral unit.)	0	0	1	$U(N+M)/U(N) \times U(M)$	$U(n)$
	BDI (chiral orthog.)	+1	+1	1	$SO(N+M)/SO(N) \times SO(M)$	$U(2n)/Sp(n)$
	CII (chiral sympl.)	−1	−1	1	$Sp(2N+2M)/Sp(2N) \times Sp(2M)$	$U(2n)/O(2n)$
BdG	D	0	+1	0	$SO(2N)$	$O(2n)/U(n)$
	C	0	−1	0	$Sp(2N)$	$Sp(n)/U(n)$
	DIII	−1	+1	1	$SO(2N)/U(N)$	$O(2n)$
	CI	+1	−1	1	$Sp(2N)/U(N)$	$Sp(n)$

# 🌟 Topological phase classification

**TABLE 2.** Summary of the *main result of this paper*: listed are again the ten symmetry classes of single particle Hamiltonians (from TABLE 1) classified in terms of the presence or absence of time-reversal symmetry (TRS) and particle-hole symmetry (PHS), as well as sublattice (or “chiral”) symmetry (SLS) [17, 18, 19]. The last three columns list all possible topologically non-trivial quantum ground states as a function of symmetry class and spatial dimension  $d$ . The symbols  $\mathbb{Z}$  and  $\mathbb{Z}_2$  indicate that the space of quantum ground states is partitioned into different topological sectors labeled by an integer ( $\mathbb{Z}$ ), or a  $\mathbb{Z}_2$  quantity (two sectors only), respectively.

System	Cartan nomenclature	TRS	PHS	SLS	$d = 1$	$d = 2$	$d = 3$
standard (Wigner-Dyson)	A (unitary)	0	0	0	-	$\mathbb{Z}$	-
	AI (orthogonal)	+1	0	0	-	-	-
	AII (symplectic)	-1	0	0	-	$\mathbb{Z}_2$	$\mathbb{Z}_2$
chiral (sublattice)	AIII (chiral unit.)	0	0	1	$\mathbb{Z}$	-	$\mathbb{Z}$
	BDI (chiral orthog.)	+1	+1	1	$\mathbb{Z}$	-	-
	CII (chiral sympl.)	-1	-1	1	$\mathbb{Z}$	-	$\mathbb{Z}_2$
BdG	D	0	+1	0	$\mathbb{Z}_2$	$\mathbb{Z}$	-
	C	0	-1	0	-	$\mathbb{Z}$	-
	DIII	-1	+1	1	$\mathbb{Z}_2$	$\mathbb{Z}_2$	$\mathbb{Z}$
	CI	+1	-1	1	-	-	$\mathbb{Z}$



# Extension to nodal superconductors

## Topological surface states in nodal superconductors

Andreas P. Schnyder

E-mail: [a.schnyder@fkf.mpg.de](mailto:a.schnyder@fkf.mpg.de)

Max-Planck-Institut für Festkörperforschung, Heißenbergstrasse 1, D-70569 Stuttgart, Germany

Philip M. R. Brydon

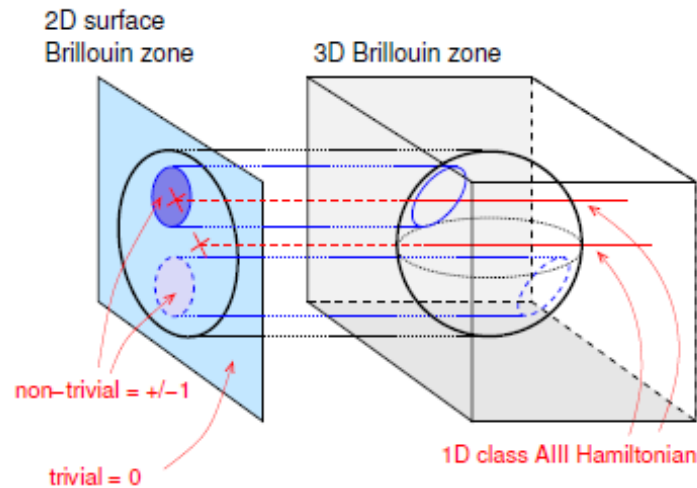
E-mail: [pbrydon@umd.edu](mailto:pbrydon@umd.edu)

Condensed Matter Theory Center, University of Maryland, College Park, MD 20742, USA

**Abstract.** Topological superconductors have become a subject of intense research due to their potential use for technical applications in device fabrication and quantum information. Besides fully gapped superconductors, unconventional superconductors with point or line nodes in their order parameter can also exhibit nontrivial topological characteristics. This article reviews recent progress in the theoretical understanding of nodal topological superconductors, with a focus on Weyl and noncentrosymmetric superconductors and their protected surface states. Using selected examples, we review the bulk topological properties of



# Edge states in bulk nodal superconductors



(from Schnyder and Brydon)

**Figure 3.** The relationship of the bulk gap structure to the surface states of a nodal topological superconductor. The left part of the figure shows the surface Brillouin zone with the projected Fermi surface indicated in black. Flat-band surface states occur within the two regions bounded by the projected nodal lines (dark blue and light gray areas). Within these two regions the winding number  $W$  takes on the values  $W = \pm 1$ , while outside these regions it is zero; the bulk Hamiltonians restricted to a surface momentum in these regions (red lines in 3D Brillouin zone) belong to symmetry class AIII and are topologically trivial and nontrivial, respectively. The right part of the figure shows the three-dimensional bulk Brillouin zone with a spherical Fermi surface (black ellipse) and two nodal rings (solid and dashed blue ellipses).



# Possible nodal topological systems

**Table 2.** List of candidate materials for nodal topological superconductivity with (majority) spin-triplet pairing. Note that in some materials the evidence is contradictory. NCS: Noncentrosymmetric superconductor. HF: Heavy fermion superconductor. FM: Ferromagnetic superconductor. NMR: Nuclear magnetic resonance. SH: Specific heat. UA: Ultrasound attenuation. TC: Thermal conductivity. PD: London penetration depth.  $H_{c2}$ : Upper critical field

Material	Type	Evidence for triplet pairing	Evidence for nodes	Probable pairing symmetry
A phase of $^3\text{He}$	superfluid	NMR, magnetiz. [53]	SH [51]	chiral
CePt <sub>3</sub> Si	NCS, HF	indirect	PD, NMR, etc. [139, 140, 141, 142]	( $s + p$ )-wave
CeIrSi <sub>3</sub> <sup>†</sup>	NCS, HF	NMR [143, 144]	NMR [143, 144]	( $s + p$ )-wave
CeRhSi <sub>3</sub> <sup>†</sup>	NCS, HF	$H_{c2}$ [145]		?
Li <sub>2</sub> Pt <sub>3</sub> B	NCS	NMR [147]	PD, NMR, SH [146, 147, 148]	( $s + p$ )-wave
LaNiC <sub>2</sub>	NCS	indirect [149]	PD [150]	nonunitary
LaNiGa <sub>2</sub>	centro.	indirect [152]		nonunitary
URhGe	FM, HF	indirect [153]	SH [154]	$p$ -wave
UCoGe	FM, HF	NMR [155]	indirect [156]	$p$ -wave
UGe <sub>2</sub> <sup>†</sup>	FM, HF	$H_{c2}$ [157, 158]	NMR [159]	$p$ -wave
UPt <sub>3</sub>	HF	NMR [160]	SH, UA, TC [161]	chiral $f$ -wave
UBe <sub>13</sub>	HF	NMR [162]	SH, NMR [163, 164]	nodal

# 🌟 Possible topological nodal systems

**Table 3.** List of candidate materials for nodal topological superconductivity with (majority) spin-singlet pairing. HF: Heavy fermion superconductor. SL: Superlattice. ARPES: Angle-resolved photoemission spectroscopy. STM: Scanning tunneling microscopy. NMR: Nuclear magnetic resonance. PD: London penetration depth. SH: Specific heat. TC: Thermal conductivity. MT: Magnetic torque. PKE: Polar Kerr effect.  $\mu$ SR: Muon spin rotation.

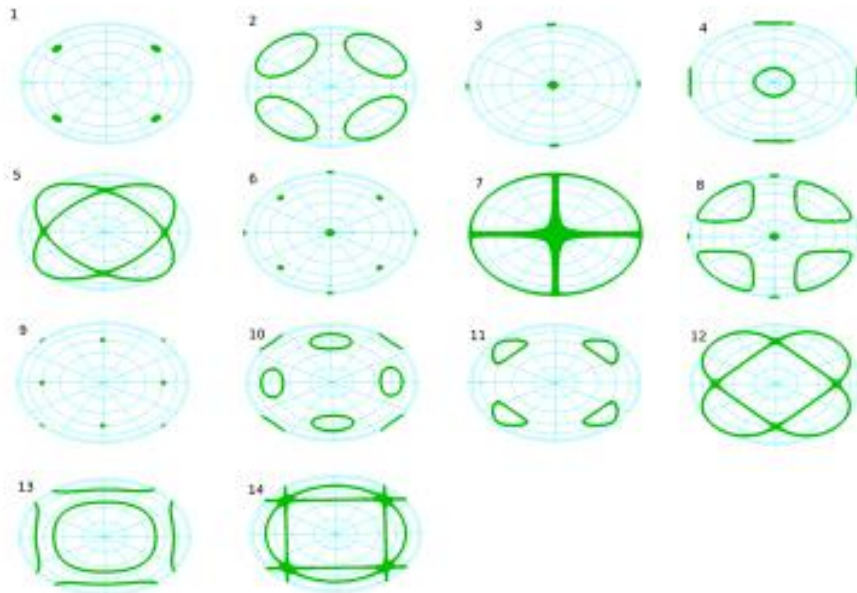
Material	Type	Time-reversal symmetry	Evidence for nodes	Probable pairing symmetry
YBa <sub>2</sub> Cu <sub>3</sub> O <sub>6+x</sub> , La <sub>2-x</sub> Sr <sub>x</sub> CuO <sub>4</sub> , etc.	high-temp. supercond.	Yes	ARPES, STM, NMR, PD, etc. [34, 35]	$d_{x^2-y^2}$ -wave
CeCu <sub>2</sub> Si <sub>2</sub>	HF	Yes	indirect [174]	$d$ -wave
CeCoIn <sub>5</sub>	HF	Yes	SH, TC, NMR, STM [36, 37, 38, 39, 175]	$d_{x^2-y^2}$ -wave
CeIrIn <sub>5</sub>	HF	Yes	SH, TC, NMR [37, 175]	$d$ -wave
CeRhIn <sub>5</sub> <sup>†</sup>	HF	Yes	SH [176]	$d$ -wave
URu <sub>2</sub> Si <sub>2</sub>	HF	No (MT [42], PKE [177])	SH, NMR, TC [40, 41]	$(d \pm id)$ -wave
SrPtAs	pnictide	No ( $\mu$ SR [46])	indirect [47]	$(d \pm id)$ -wave
CeCoIn <sub>5</sub> /YbCoIn <sub>5</sub>	SL		indirect [178]	likely $d$ -wave
Cu <sub>x</sub> (PbSe) <sub>5</sub> (Bi <sub>2</sub> Se <sub>3</sub> ) <sub>6</sub>	SL		SH [179]	line node

<sup>†</sup> superconducting under pressure

# Example of model with bulk topological phases

Cubic noncentrosymmetric superconductors, eg  $\text{Li}_2\text{Pd}_x\text{Pt}_{3-x}\text{B}$

- Spin-orbit interaction mixes singlet and triplet pairing, leading to an exotic array of possible energy gaps on the Fermi surface



As gap parameters change nodes on bulk Fermi surface appear and disappear

The fully gapped states can be classified by topological numbers

The non-trivial ones will have edge states

# 🔥 Recap of tour around topics in topological superconductors

- The 2016 Nobel prize
- The Quantum Hall effect
- Topological Insulators
- Unconventional superconductivity in  $\text{Sr}_2\text{RuO}_4$
- Kerr effect in  $\text{Sr}_2\text{RuO}_4$
- Superfluid angular momentum and orbital magnetization of  $\text{Sr}_2\text{RuO}_4$
- Ten fold classification of topological systems
- Topology in nodal superconductors

